Increase in pulmonary blood flow at birth: role of oxygen and lung aeration

Justin A.R. Lang[1,2], James T. Pearson[3,4], Corinna Binder-Heschl[1,2,5], Megan J. Wallace[1,2], Melissa L. Siew[1,2], Marcus J. Kitchen[6], Arjan B. te Pas[7], Andreas Fouras[8], Robert A. Lewis[9,10], Graeme R. Polglase[1,2], Mikiyasu Shirai[11] and Stuart B. Hooper[1,2]

[1] *The Ritchie Centre, Hudson Institute of Medical Research, Melbourne, Australia*
[2] *Department of Obstetrics and Gynaecology, Monash University, Melbourne, Australia*
[3] *Monash Biomedical Imaging Facility and Department of Physiology, Monash University, Melbourne, Australia*
[4] *Australian Synchrotron, Melbourne, Australia*
[5] *Medical University of Graz, Austria*
[6] *School of Physics and Astronomy, Monash University, Melbourne, Australia*
[7] *Department of Pediatrics, Leiden University Medical Centre, Leiden, Netherlands*
[8] *Department of Mechanical and Aerospace Engineering, Monash University, Melbourne, Australia*
[9] *Medical Imaging and Radiation Sciences, Monash University, Melbourne, Australia*
[10] *Department of Medical Imaging, University of Saskatchewan, Saskatoon, Canada*
[11] *Department of Cardiac Physiology, National Cerebral and Cardiovascular Center Research Institute, Osaka, Japan*

Key points

- There is no well-established, direct correlation between local aeration and perfusion in the lungs immediately following birth.
- In a new study of simultaneous X-ray imaging and angiography in near-term rabbits, we investigated the relative contributions of lung aeration and increased oxygenation in the increase in pulmonary perfusion at birth.
- We demonstrated that partial lung aeration induces a global increase in pulmonary blood flow that is independent of changes in inspired oxygen.
- These results show that mechanisms unrelated to oxygenation or the spatial relationships that match ventilation to perfusion initiate the large increase in pulmonary blood flow at birth.

Abstract Lung aeration stimulates the increase in pulmonary blood flow (PBF) at birth, but the spatial relationships between PBF and lung aeration and the role of increased oxygenation remain unclear. Using simultaneous phase-contrast X-ray imaging and angiography, we have investigated the separate roles of lung aeration and increased oxygenation in PBF changes at birth using near-term (30 days of gestation) rabbit kits ($n = 18$). Rabbits were imaged before ventilation, then the right lung was ventilated with 100% nitrogen (N_2), air or 100% O_2 (oxygen), before all kits were switched to ventilation in air, followed by ventilation of both lungs using air. Unilateral ventilation of the right lung with 100% N_2 significantly increased heart rate (from 69.4 ± 4.9 to 93.0 ± 15.0 bpm), the diameters of both left and right pulmonary axial arteries, number of visible vessels in both left and right lungs, relative PBF index in both pulmonary arteries, and reduced bolus transit time for both left and right axial arteries (from 1.34 ± 0.39 and 1.81 ± 0.43 s to 0.52 ± 0.17 and 0.89 ± 0.21 s in the left and right axial arteries, respectively). Similar changes were observed with 100% oxygen, but increases in visible vessel number and vessel diameter of the axial arteries were greater in the ventilated right lung during unilateral ventilation. These findings confirm that PBF increase at birth is not spatially related to lung aeration and that the increase in PBF to unventilated regions is unrelated to oxygenation, although oxygen can potentiate this increase.

 DOI: 10.1113/JP270926

The Journal of Physiology

(Received 13 May 2015; accepted after revision 4 August 2015; first published online 17 August 2015)
Corresponding author Prof. S. Hooper: The Ritchie Centre, Hudson Institute of Medical Research, 27–31 Wright Street, Clayton, 3168, Victoria, Australia. Email: Stuart.Hooper@monash.edu

Abbreviations ET, endotracheal tube; ID, internal diameter; MPA, main pulmonary artery; PC, phase contrast; PBF, pulmonary blood flow; PVR, pulmonary vascular resistance.

Introduction

The increase in pulmonary blood flow (PBF) at birth underpins the circulatory transition that is critical for postnatal survival (Iwamoto *et al.* 1987). Shifting the site of gas exchange from the placenta to the lungs requires aeration of the lung and a reduction in pulmonary vascular resistance (PVR) to increase pulmonary perfusion (Rudolph, 1979; Berhrsin & Gibson, 2011). This is not only necessary for efficient pulmonary gas exchange but also restores venous return to the heart, which is markedly reduced following umbilical cord clamping (Rudolph, 1979; Crossley *et al.* 2009; Bhatt *et al.* 2013). The increase in PBF at birth is thought to result from an integration of multiple mechanical and vasoactive factors acting in concert and, until recently, was assumed to occur in a spatially dependent manner as lung regions aerated (Morin & Egan, 1992; Gao & Raj, 2010). Although the temporal relationship between lung aeration and the rapid increase in PBF at birth is well established (Teitel *et al.* 1990; Polglase & Hooper, 2006), recent findings suggest there is no simple, direct correlation between local aeration and perfusion (Lang *et al.* 2014).

The factors contributing to the high PVR *in utero* are thought to include high intraluminal pressures induced by airway liquid accumulation and relatively low fetal oxygen tensions, resulting in sustained vasoconstriction of the pulmonary vasculature (Morin & Egan, 1992; Polglase & Hooper, 2006). As the developing pulmonary vasculature becomes sensitive to small changes in oxygen tension from about mid-gestation (Lewis *et al.* 1976; Blanco *et al.* 1988; Morin & Egan, 1992), increased oxygenation at birth is widely regarded as a major driver of pulmonary vasodilatation at birth. Indeed, alteration in oxygen tension is a well-known mediator of ventilation/perfusion relationships in the adult lung (Weissmann *et al.* 2006; Sylvester *et al.* 2012). Oxygen (O_2) stimulates vasodilatation directly via mitochondria, as well as through vasodilator intermediates including nitric oxide (NO) (Tiktinsky & Morin, 1993), the vasodilatory prostaglandins PGI_2 (prostacyclin) and PGE_2, bradykinin and purine nucleotides (Gao & Raj, 2010). However, despite the well-known role for O_2, ventilation with a hypoxic gas mixture is able to elicit the majority (60%) of the breathing-related increase in PBF at birth (Teitel *et al.* 1990). Similarly, both increases and decreases in oxygenation status are associated with ventilation-induced increases in PBF that are identical in magnitude at birth (Sobotka *et al.* 2011). While the precise mechanisms are unclear, it is clear that the initial entry of gas into the lungs is the most significant factor responsible for the increase in PBF at birth.

Our recent study has demonstrated that the increase in PBF at birth is not spatially related to lung aeration as partial lung aeration caused a global increase in PBF (Lang *et al.* 2014). It was expected that regional lung aeration would cause localized reductions in PVR through (i) an increase in oxygenation and (ii) capillary expansion and recruitment due to an increase in alveolar/capillary wall transmural pressures resulting from a surface tension-mediated increase in lung recoil (Hooper, 1998). As neither mechanism was expected to be active in non-ventilated lung regions, the finding that the increase in PBF is not spatially related to lung aeration (Lang *et al.* 2014) indicates that the mechanisms responsible for the increase in PBF at birth require re-evaluation. It is possible that regional lung aeration increased levels of circulating partial pressure of oxygen in arterial blood (P_{aO_2}), causing vasodilatation in non-aerated lung regions. Our aim was to examine this hypothesis by partially aerating the lung in the absence of O_2, and determine the effect on PBF in unaerated lung regions. We hypothesized that partial lung aeration with 100% nitrogen (N_2) (0% oxygen) would trigger a global increase in PBF and increasing O_2 levels in the inspired gas would enhance the increase in PBF in aerated regions. To assess the regional changes in PBF and the spatial relationships between PBF and lung aeration, we used our previously established imaging technique that combines phase-contrast (PC) X-ray imaging with angiography in near-term rabbit neonates.

Methods

Experimental procedure

All animal procedures were approved by the SPring-8 Animal Care and Monash University's School of Biomedical Science's Animal Ethics Committees and the Japan Synchrotron Radiation Research Institute, SPring-8 Animal Experiment Committee (proposals 2012A0047, 2012A1314). All studies were conducted in experimental hutch 3 of beamline 20B2, in the Biomedical Imaging Centre at the SPring-8 synchrotron, Japan.

Pregnant New Zealand white rabbits at 30 days of gestation (term ≈ 32 days) were anaesthetized using propofol (I.V.; 12 mg kg^{-1} bolus; Rapinovet, Schering-Plough Animal Health, Tokyo, Japan) and intubated. Anaesthesia was maintained by isoflurane inhalation (1.5–4%; Isoflu, Dainippon Sumitomo Pharma Co., Osaka, Japan). Fetal rabbits ($n = 18$) were partially delivered by caesarean section, sedated with sodium pentobarbitone (13 mg kg^{-1} I.P.; Somnopentyl, Kyoritsu Seiyaku Co., Ltd, Tokyo, Japan) and a jugular vein catheter (24 G Intracath, Becton Dickinson, Franklin Lakes, NJ, USA) and an endotracheal (ET) tube (18 G Intracath; via tracheostomy) were inserted. The tip of the ET tube was directed into the right bronchus so that with ventilation onset only the right lung was ventilated (unilateral ventilation). During the surgical procedure, the kit's head remained covered with fetal membranes to prevent lung aeration, the umbilical cord remained intact and the ET tube was obstructed to prevent breathing. The kits were then delivered and the umbilical cord was ligated before they were placed upright in an acrylic frame. ECG leads were attached to the skin of the upper limb and both lower limbs. The ET tube was then connected to a purpose-built, time-cycled, pressure-controlled ventilator (Kitchen *et al.* 2010) and image acquisition began as soon as possible after the kits were positioned. Kits were initially ventilated in either 100% N_2, 21% O_2 (air) or 100% O_2 using a peak inflation pressure of 25 cmH_2O and a positive end-expiratory pressure of 5 cmH_2O. At the conclusion of the experiment (~10 min after ventilation onset for kits), all animals were humanely killed with an overdose of sodium pentobarbitone (Pentobarbital; > 100 mg kg^{-1}) administered I.V. (doe) or I.P. (kits).

X-ray and angiography imaging

Monochromatic X-rays at 33.2 keV and a photon flux of $\sim 10^8$ photons mm^{-2} s^{-1} was used for imaging with the kits positioned 1.0 m upstream of the detector. The scientific-CMOS (sCMOS) detector (pco.edge; PCO AG, Kehlheim, Germany) was coupled to a 25 μm thick gadolinium oxysulfide (Gd_2O_2S:Tb+) powdered phosphor and a tandem lens system that provided an effective pixel size of 15.3 μm and an active field of view of 29 (W) × 30 (H) mm^2. Images were acquired at a frame rate of 10 Hz. During imaging, iodine boluses (Iomeron 350 mg ml^{-1} iodine; Bracco-Eisai Pty. Ltd, Tokyo, Japan; 1.5 μl per gram kit body weight at 11 ml s^{-1}) were administered via the jugular vein using a remote-controlled syringe pump (PHD2000, Harvard Apparatus Inc., Holliston, MA, USA). Iodine boluses were injected and images were acquired for an average of 44 ± 9 s before ventilation onset and for a further 97 ± 14 s during unilateral ventilation of the right lung with either 100% N_2 ($n = 6$), 21% O_2 ($n = 6$) or 100% O_2 ($n = 6$). Following this period, unilateral ventilation continued in air in all groups for 184 ± 14 s, after which the ET tube was retracted to ventilate both lungs in air, which continued for 118 ± 12 s. The elapsed time between ventilation periods was consistent between groups.

Image analysis

Images were analysed using ImageJ (v1.49; NIH, Bethesda, MD, USA) as described previously (Lang *et al.* 2014). Comparisons were made between the number of visible pulmonary vessels, vessel diameters, heart rate, iodine ejection per beat, pulmonary transit time and change in mean grey level profiles within the left and right main axial arteries and the aorta following iodine injection. When ECG recordings were unsuccessful, heart rate was calculated from the inter-beat interval derived from the imaging sequence.

Vessel quantification

Visible blood vessels were counted using a composite image constructed from 10 X-ray image frames (1 s) of peak opacification during an iodine bolus (Lang *et al.* 2014). Images acquired during lung movement were excluded due to motion blur. Iodine-perfused arterial vessels distal to branching points were counted as individual vessels and were visible up to the third order of branching.

Main axial artery vessel diameter

Changes in pixel grey level (intensity) along virtual lines transecting vessels perpendicular to a vessel wall were used to measure vessel internal diameter (ID). Line profiles were drawn over the left and right main axial arteries (taken mid-lung at the seventh intercostal space), tracking ID changes from the baseline pre-ventilation period (Lang *et al.* 2014). To correct for background variation, during iodine perfusion line profiles were divided by the average background intensity, over the 10 frames (1 s) immediately prior to the first appearance of contrast within the vessel. Internal vessel edges were determined as the first pixel to drop below one standard deviation of the mean intensity of the background tissue at either end of the line profile (~5 pixels past the vessel edge). Vessel diameters measured in pixels from each frame were averaged over five frames (0.5 s) then multiplied by the known pixel size (15.3 μm) to estimate a mean vessel ID.

Pulmonary arterial transit time

A virtual box was placed over the distal end of the left and right main axial arteries before first-order branching (taken at the level of the eighth intercostal space for consistency). The mean intensity of this region was calculated for each frame. Bolus arrival time was designated as the frame in which half of the peak opacity (maximum % change from background) is reached for the first time (half-peak opacity), which corrects for problems due to steady state peak opacity values in cases of poor wash-out (Shpilfoygel *et al.* 2000). The elapsed time between the half-peak opacity value in the main pulmonary artery (MPA) compared to the left and right axial arteries (at the eighth intercostal space) was calculated to give an approximation of bolus pulmonary artery transit time.

Changes in opacity over time within the MPAs and aorta

A virtual box was placed over the MPA immediately distal to the right ventricular outlet, the descending aorta, and the left and right main axial arteries at the level of the seventh intercostal space, the last providing a centrally located, clear and unobstructed view of the large conduit arteries during both the pre-ventilation and the ventilation imaging time periods. The changes in mean intensity within each box were plotted against time as a percentage change from background levels (mean background intensity averaged over 10 frames before iodine injection) throughout each iodine injection sequence. The maximum of this time–opacity curve was then divided by the pulmonary arterial transit time to provide an indicator of changes in pulmonary arterial flow in both lungs, right ventricular output and the relative contribution of right ventricular output to flow in the aorta during all ventilation periods.

Statistical analysis

Changes in visible vessel number, blood vessel ID, heart rate, pulmonary arterial transit time and opacity of blood vessels were analysed using a two-way repeated measures ANOVA. Post-hoc analysis used the Holm–Sidak method. A P value of < 0.05 was considered statistically significant.

Results

Animal data

PC X-ray images were obtained from 18 kits (30 days gestational age) from eight pregnant rabbits. Mean kit weight was 42.3 ± 1.3 g, which was similar between groups.

Observations from PC X-ray videos

Consistent with our previous findings (Lang *et al.* 2014), unilateral ventilation of the right lung ($1LV_1$) markedly increased iodine flow into both left (unaerated) and right (aerated) axial arteries compared to the pre-ventilation period (0LV). The increase in flow in the unaerated lung was similar irrespective of whether the initial gas used to ventilate the right lung was 100% N_2 (Fig. 1; Supplementary Video S1), air (Lang *et al.* 2014) or 100% O_2 (Fig. 1; Supplementary Video S2). As such, iodine distribution increased to the non-aerated left lung despite ventilation with a gas mixture that had no oxygen. Continued unilateral ventilation in air ($1LV_2$) and subsequent ventilation of both lungs with air (2LV) sustained this increase in PBF and appeared to cause only modest (potentially time-related) increases compared to the initial increase in PBF in all groups (Fig. 1).

Indices of vessel recruitment

Following unilateral ventilation of the right lung with 100% N_2 ($1LV_1$ in Fig. 2), the total number of visible vessels increased in the left and right lungs respectively from 21 ± 5 and 19 ± 5 to 45 ± 4 and 44 ± 4 following ventilation onset. Similarly, unilateral ventilation of the right lung with air increased the number of visible vessels from 28 ± 5 and 28 ± 6 to 48 ± 9 and 45 ± 8 in the left and right lungs, respectively; the percentage increase was similar to ventilation with 100% N_2. Unilateral ventilation with 100% O_2 ($1LV_1$) increased vessel numbers from 34 ± 6 and 33 ± 5 to 65 ± 7 and 79 ± 8 in left and right lungs, respectively. While unilateral ventilation of the right lung with 100% N_2 and air increased visible vessel numbers similarly in both left and right lungs, ventilation with 100% O_2 resulted in a greater increase in the ventilated right lung (79 ± 8 vessels in the right lung compared to 66 ± 7 vessels in the unventilated left lung). Following the period of unilateral ventilation with 100% N_2, unilateral ventilation of the right lung ($1LV_2$) and then bilateral ventilation (2LV) with air increased the number of visible vessels further to 56 ± 5 and 62 ± 7 in the left and right lungs, respectively. Similarly, following the period of unilateral ventilation with air and 100% O_2, the subsequent ventilation periods of unilateral ventilation with air and bilateral ventilation with air tended to increase the number of visible vessels further, but this increase was not significant.

Heart rate and opacity changes in the MPA and aorta over time

Heart rate increased from 69.4 ± 4.9 to 93.0 ± 15.0 bpm following unilateral ventilation of the right lung with 100% N_2. Similarly, unilateral ventilation of the right lung with air or 100% O_2 increased heart rates from 55 ± 5 and 46.4 ± 3.3 bpm to 90.3 ± 13.4 and 73.0 ± 10.0 bpm, respectively (Fig. 3*A*). Heart rates were not significantly changed during the subsequent period of unilateral lung ventilation with air in all groups ($1LV_2$), but increased further to 136.0 ± 15.2, 129.9 ± 7.0 and 115.6 ± 10 bpm during bilateral ventilation (2LV) in pups initially ventilated with 100% N_2, air and 100% O_2, respectively. No differences in heart rate were detected between groups.

Peak opacity within the MPA (Fig. 3*B*), which provides an indicator of right ventricle output, increased significantly following unilateral ventilation of the right lung with either air or 100% O_2. Unilateral ventilation of the right lung with air increased peak opacity from 39.9 ± 7.3 to 72.8 ± 4.4% above background, whereas unilateral ventilation of the right lung with 100% O_2 increased peak opacity from 35.5 ± 6.1 to 64.2 ± 5.6% above background; these values did not increase further after continued ventilation ($1LV_2$ or 2LV). Unilateral ventilation of the right lung with 100% N_2 also tended to increase MPA peak opacity, from 31.3 ± 5.6 to 45.8 ± 7.0% above background, but this increase only became statistically significant after the switch to air ($1LV_2$), when it increased to 57.3 ± 2.8% above background; this did not significantly increase further with continued ventilation (2LV). Peak opacification in the descending aorta (Fig. 3*C*), representing the contrast agent diverted through the ductus arteriosus, increased significantly in response to unilateral ventilation when ventilated with either air or 100% O_2 but did not significantly increase further with continued ventilation.

Arterial vessel internal diameter

Compared to pre-ventilation values, unilateral ventilation ($1LV_1$) of the right lung significantly increased ID of the left and right main axial arteries at the level of the seventh intercostal space in both lungs in all three groups (Fig. 4). The diameters increased from 533 ± 40 and 533 ± 35 μm in the left and right main axial arteries to 597 ± 39 and 596 ± 40 μm, respectively, in response to unilateral ventilation of the right lung with 100% N_2. These increases were similar to those observed following unilateral ventilation with air (increased from 505 ± 49 and 505 ± 39 μm to 585 ± 58 and 581 ± 40 μm, in left and right vessels, respectively) and 100% O_2 (increased from 500 ± 58 and 506 ± 55 μm to 559 ± 47 and 651 ± 56 μm in left and right vessels, respectively), except that the increase in the right axial artery ventilated with 100% O_2 tended to be greater. While ID tended to increase during the subsequent ventilation periods, this increase was not significant. IDs between the groups were not significantly different at any point although IDs in the right lung following initial ventilation with O_2 tended to be greater.

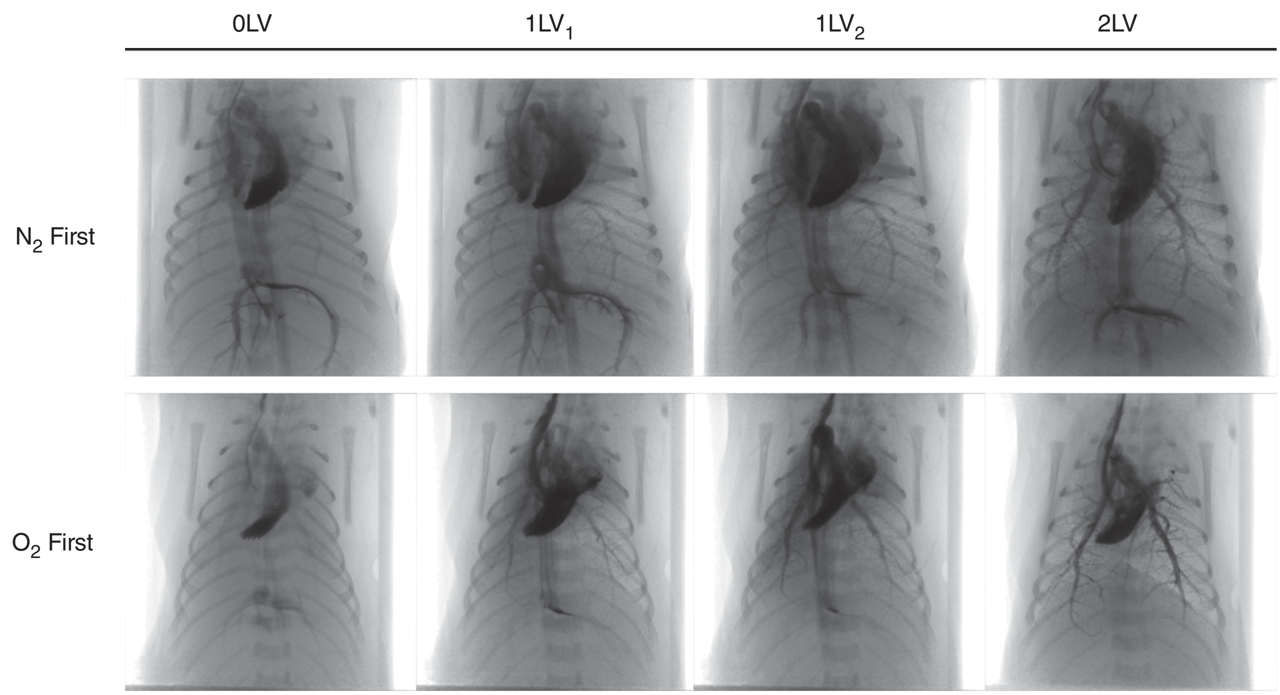

Figure 1. PC X-ray and angiography images
Representative X-ray image sequences of newborn rabbits imaged prior to ventilation (0LV), following unilateral ventilation of the right lung ($1LV_1$) with either 100% N_2 or 100% O_2, subsequent ventilation with air (21% O_2) in all kits ($1LV_2$), and later ventilation of both lungs in air (2LV). Images were obtained 1–3 s following iodine bolus injection.

Iodine bolus transit time

Pulmonary arterial transit time, given by the elapsed time between iodine bolus passage from the MPA to arrival at the distal end of the left and right axial arteries, decreased significantly in response to unilateral ventilation ($1LV_1$) in all groups irrespective of the gas used (100% N_2, air or 100% O_2) (Fig. 5*A*). Unilateral ventilation of the right lung with 100% N_2 decreased the transit time from 1.34 ± 0.39 and 1.81 ± 0.43 s to 0.52 ± 0.17 and 0.89 ± 0.21 s in the left and right pulmonary arteries, respectively. Similarly, unilateral ventilation with 100% O_2 decreased the transit times from 1.33 ± 0.41 and 1.45 ± 0.28 s to 0.23 ± 0.06 and 0.33 ± 0.14 s in the left and right axial arteries, respectively. Subsequent ventilation periods ($1LV_2$, 2LV) did not significantly alter the transit time from the initial decrease and no difference was detected between lungs or between groups.

Changes in relative PBF indices

Relative PBF indices, given by the maximum change in relative iodine levels (% decrease in intensity below background) divided by the arterial transit time, increased significantly in response to unilateral ventilation in all groups irrespective of the gas used (100% N_2, air or 100% O_2) (Fig. 5*B*). Unilateral ventilation of the right lung with 100% N_2 increased the relative PBF index from 6.0 ± 2.9 and 5.5 ± 2.6% s^{-1} to 51.0 ± 25.1 and 69.7 ± 25.4% s^{-1} in the left and right pulmonary arteries, respectively. Unilateral ventilation of the right lung with air increased relative PBF index from 13.8 ± 6.2 and 6.9 ± 2.3% s^{-1} to 78.0 ± 32.0 and 61.1 ± 22.1% s^{-1} in the left and right pulmonary arteries, respectively. Unilateral ventilation of the right lung with 100% O_2 increased relative PBF index from 8.1 ± 3.2 and 8.3 ± 2.4% s^{-1} to 105.5 ± 27.8 and 98.7 ± 20.4% s^{-1} in the left and right pulmonary arteries, respectively. The subsequent ventilation period ($1LV_2$) did not significantly alter the relative PBF values in any group but relative PBF increased significantly after changing to bilateral ventilation (2LV). No difference was detected between lungs or between groups.

Discussion

The recent finding that partial lung aeration causes a global increase in lung perfusion indicates that pulmonary vasodilatation at birth is not spatially related to lung aeration and that an additional, previously unsuspected mechanism may be involved (Lang *et al.* 2014). However, the possibility of re-circulation of oxygenated blood-causing increased oxygenation and vasodilatation in these unventilated lung regions could not be completely dismissed. The data presented in this study now confirm that the global increase in PBF that is initiated by partial lung aeration immediately following birth is independent of changes in oxygenation. However, inhalation of 100% oxygen was found to have an additive effect on pulmonary vasodilatation and PBF, which was localized to aerated lung regions. This indicates that there are a number of factors that work independently to increase PBF at birth.

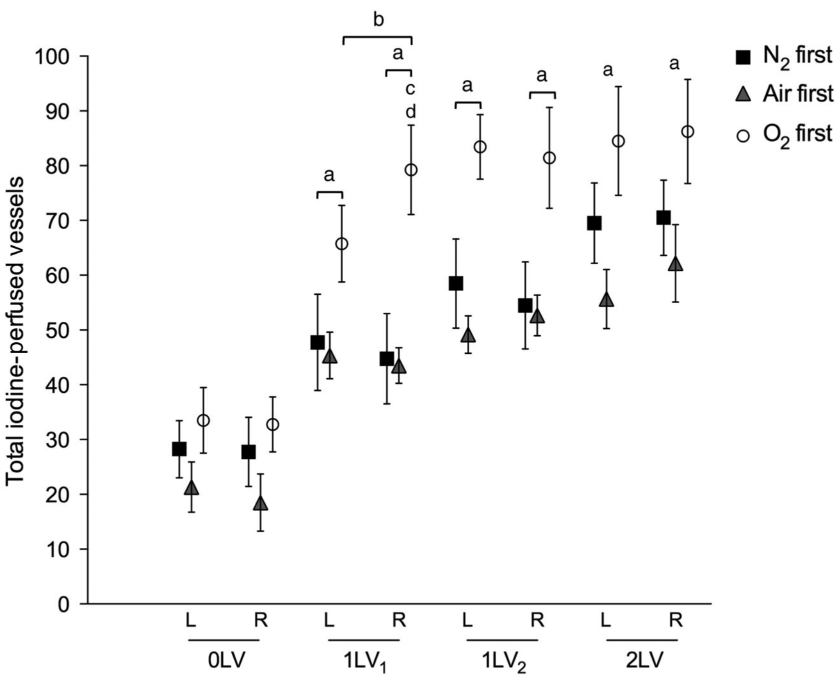

Figure 2. Changes in visualized blood vessel number
Mean iodine-perfused vessel number (±SEM) in the left and right lungs at each ventilation period (0LV, $1LV_1$, $1LV_2$ and 2LV) in the N_2 first (black solid squares), air first (grey solid triangles) and O_2 first (open circles) groups. [a]$P < 0.05$ compared to baseline (0LV) in the same lung in all groups; [b]$P < 0.05$ left lung *vs.* right lung in O_2 first; [c]$P < 0.05$ air first *vs.* O_2 first; [d]$P < 0.05$ N_2 first *vs.* O_2 first.

In this study, partial aeration of the right lung was confirmed by PC X-ray imaging, which gives rise to a distinctive speckle pattern caused by multiple phase shifts at the air/liquid boundaries in the distal airways (Kitchen *et al.* 2004). As such, we are able to confirm from the images the lack of aeration in lung regions not being ventilated. Findings were consistent with previous studies, showing that a significant ventilation/perfusion mismatch occurs after birth when the lung is partially aerated (Fig. 1; Supplementary Videos S1 and S2) (Lang *et al.* 2014). This observation has been extended to show that unilateral ventilation of near-term newborn rabbit kits with an oxygen-free inspired gas also causes a global increase in PBF. We consistently found that, in all parameters measured, the greatest change occurs between the pre-ventilation and the initial unilateral ventilation periods, with relatively minor changes occurring thereafter. This indicates that partial lung aeration induces a large global increase in PBF, which is mediated by a potent mechanism that is unrelated to oxygenation levels.

As pulmonary perfusion is low prior to lung aeration (Rudolph, 1979; Crossley *et al.* 2009), the number of visible vessels and the penetration of contrast agent into distal vessels is low and the transit time for the flow of contrast through the pulmonary vessels is long. Following partial lung aeration, irrespective of the inspired gas content, the number of visible vessels, the diameter of the pulmonary vessels and the penetration of contrast agent into the distal pulmonary vasculature tree increased, and transit time for the flow of contrast agent markedly decreased (Fig. 1; Supplementary Videos S1 and S2). These changes are all indicative of downstream vasodilatation, vessel recruitment and an associated fall in PVR. This confirms the role of initial lung aeration as the primary stimulus for the increase in PBF at birth, although the precise mechanism involved remains intriguing. Indeed,

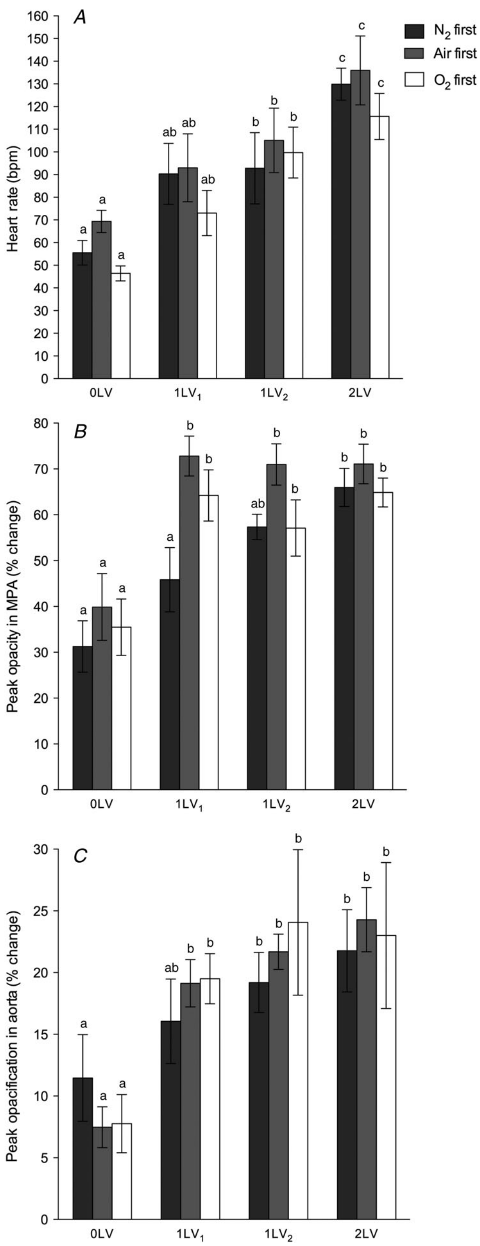

Figure 3. Heart rate and iodine distribution changes during ventilation
A, heart rate (bpm). *B*, an index of right ventricle output given by peak opacification (% intensity change from background) in the MPA (immediately distal to the right ventricle).*C*, peak opacification (% intensity change from background) in the descending aorta. In all panels data shown are mean ± SEM at each ventilation period (0LV, $1LV_1$, $1LV_2$ and 2LV) in the N_2 first (dark bars), air first (grey bars) and O_2 first (white bars) groups. Within each graph, bars that do not share a letter are significantly different from each other ($P < 0.05$).

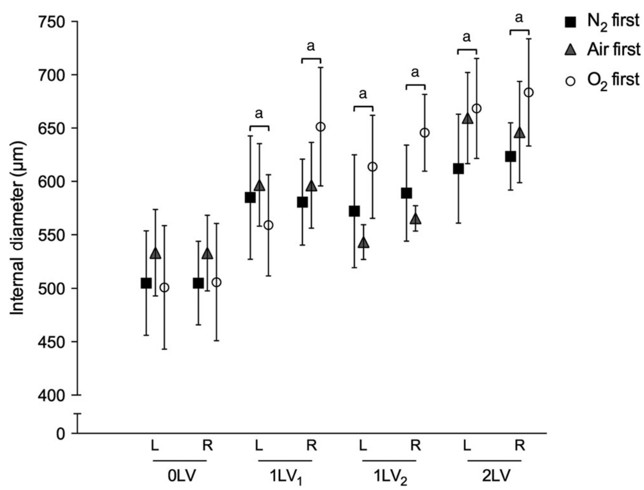

Figure 4. Blood vessel internal diameter changes during ventilation
Mean internal diameter (μm,± SEM) of the left and right axial arteries at the seventh intercostal space at each ventilation period (0LV, $1LV_1$, $1LV_2$ and 2LV) in the N_2 first (black solid squares), air first (grey solid triangles) and O_2 first (open circles) groups. $^aP < 0.05$ compared to baseline (0LV) in the same lung in the same group.

this mechanism is independent of oxygenation, but may be enhanced by oxygen, and while it can be activated by aeration of localized regions, it is translated into a global vasodilatory response. We speculate that, with gas entry into the lungs, the rapid lung liquid accumulation in the interstitial tissue (Bland *et al.* 1980; Siew *et al.* 2009) may be the stimulus for these changes, possibly via activation of J-receptors. These receptors, located within the alveolar walls, are known to respond to fluid accumulation, particularly pulmonary oedema, and signal via vagal C-fibres to cause global pulmonary vasodilatation (Paintal, 1969).

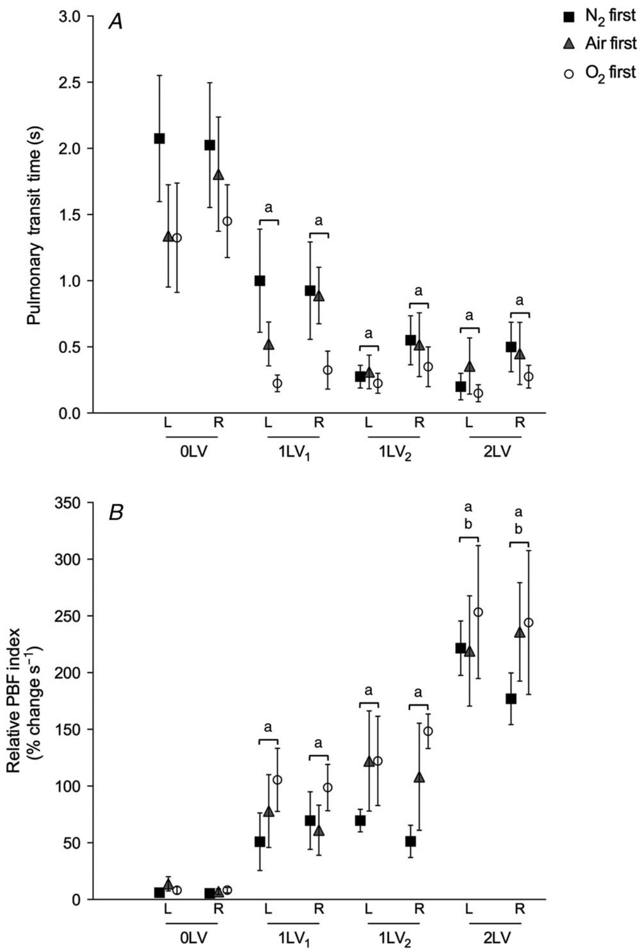

Figure 5. Indices of pulmonary blood flow changes during ventilation
A, mean arterial transit time (s,± SEM) in the left and right lungs. *B*, maximum percentage change grey value in the left and right main axial arteries at the seventh intercostal space divided by the arterial transit time (% change s^{-1} ± SEM). Data shown are at each ventilation period (0LV, 1LV$_1$, 1LV$_2$ and 2LV) in N_2 first (solid squares), air first (crosses) and O_2 first (open circles) groups. $^aP < 0.05$ compared to baseline (0LV) in the same lung in the same group; $^bP < 0.05$ compared to single-lung ventilation (both 1LV$_1$ and 1LV$_2$) in the same lung in the same group.

Unilateral ventilation of the right lung with 100% O_2 caused a greater increase in the number of visible vessels and vessel ID in the ventilated right lung compared to the unventilated left lung. As these differences between the left and right lungs were not evident in kits ventilated with 100% N_2 or air, this difference probably reflects an oxygen-dependent effect. However, the vasodilatatory effect of oxygen appeared to be localized to aerated lung regions and was additive to the effect of lung aeration with any gas. This provides further evidence to suggest that the initial effect of lung aeration on the global increase in PBF is mediated by factors that are independent of oxygen. This suggestion is consistent with previous findings that ventilation with a hypoxic gas mixture can increase PBF in sheep without an increase in oxygenation (Teitel *et al.* 1990). Similarly, the increase in PBF with ventilation onset was shown to be similar between two groups of neonatal lambs, despite the fact that oxygenation increased in one group, but decreased in the other compared to fetal levels (Sobotka *et al.* 2011). In this study, an effect of local oxygen concentration is seen; however, the majority of the differences we observed derive from the initial entry of gas into the lungs after birth, irrespective of the gas content.

The increase in cardiac function in response to unilateral ventilation, as shown by the increase in heart rate and right ventricle output, probably also contributes to the increase in PBF observed (Fig. 3). This is possible directly via the pulmonary arteries, or indirectly via an increase in aortic pressure from the increased left ventricle function, thereby supporting the increase in PBF via the patent ductus arteriosus.However, this increase in cardiac output is also dependent upon an increase in PBF. As the umbilical circulation provides a large component of the venous return and preload for both left and right ventricles, when the umbilical cord is clamped at birth, cardiac output can decrease by up to 50% (Crossley *et al.* 2009; Bhatt *et al.* 2013). Venous return is only restored after birth following lung aeration and the increase in PBF, which takes over the role of supplying preload for the left ventricle (Crossley *et al.* 2009; Bhatt *et al.* 2013). As such, the increase in PBF at birth is vital for sustaining cardiac output after birth. Interestingly, an increase in cardiac output was observed (Fig. 3*A*) in response to unilateral ventilation of the right lung with 100% N_2 (Fig. 3). As the increase in cardiac output could not be due to increased oxygenation, it can only have resulted from an increase in PBF leading to an increase in ventricular preload (Sylvester *et al.* 2012). As such, we postulate that the increase in cardiac function at birth in humans is mostly a consequence of the increase in PBF, which may be a result of an increase in oxygenation. This underpins the importance of lung aeration as the defining event that initiates the cascade of changes that characterize the transition from fetal to newborn life at birth. It not only allows gas exchange to commence and stimulates an increase in

PBF, but it also increases cardiac output by restoring the venous return lost by cord clamping.

Although the increases in main axial artery IDs induced by lung aeration were modest (increase by ∼10%; Fig. 4), because the resistance decreases exponentially with increasing vessel radius (resistance ≈ 1/radius^4), such increases in diameter reflect large decreases in resistance (Fig. 5). This is consistent with the finding of markedly reduced pulmonary transit times, which is an index of flow velocity, resulting from the decrease in PVR, although an increase in cardiac output may also have contributed. Nevertheless, unilateral ventilation with 100% N_2 both increased vessel diameter and reduced pulmonary transit times. While the decrease in transit times were not different at any point between groups, kits ventilated with 100% O_2 rapidly hit the maximum detection velocity as determined by the 10 Hz frame rate. As such, the reduction in transit times in this group may have been underestimated and may explain why a left/right difference was not observed in this parameter. Nonetheless, the rapid increase in flow velocity to both lungs and the large increase in relative PBF index (Fig 5*B*) provide a robust indication of the increase in PBF associated with lung aeration.

In fetal life, the maintenance of a high PVR restricts perfusion of non-aerated lungs, whereas at birth, lung aeration rapidly decreases PVR resulting in a large increase in PBF so that gas exchange can commence (Fineman *et al.* 1995). This study confirms that lung aeration and the increase in PBF are not spatially related and that limited aeration of the lungs leads to global PBF changes (Lang *et al.* 2014). Furthermore, we have now shown that partial aeration of the lung with a gas that has no oxygen can activate a global decrease in PVR. This indicates that a highly potent stimulus that is unrelated to oxygen can initiate the aeration-induced changes in PBF; however, the underlying mechanisms are currently unknown and require further investigation.

References

Berhrsin J & Gibson A (2011). Cardiovascular system adaptation at birth. *Paediatr Child Health* **21**, 1–6.

Bhatt S, Alison BJ, Wallace EM, Crossley KJ, Gill AW, Kluckow M, te Pas AB, Morley CJ, Polglase GR & Hooper SB (2013). Delaying cord clamping until ventilation onset improves cardiovascular function at birth in preterm lambs. *J Physiol* **591**, 2113–2126.

Blanco C, Martin C, Rankin J, Landauer M & Phernetton T (1988). Changes in fetal organ flow during intrauterine mechanical ventilation with or without oxygen. *J Dev Physiol* **10**, 53–62.

Bland R, McMillan D, Bressack M & Dong L (1980). Clearance of liquid from lungs of newborn rabbits. *J Appl Physiol* **49**, 171–177.

Crossley KJ, Allison BJ, Polglase GR, Morley CJ, Davis PG & Hooper SB (2009). Dynamic changes in the direction of blood flow through the ductus arteriosus at birth. *J Physiol* **587**, 4695–4704.

Fineman JR, Soifer SJ & Heymann MA (1995). Regulation of pulmonary vascular tone in the perinatal period. *Annu Rev Physiol* **57**, 115–134.

Gao Y & Raj JU (2010). Regulation of the pulmonary circulation in the fetus and newborn. *Physiol Rev* **90**, 1291–1335.

Hooper SB (1998). Role of luminal volume changes in the increase in pulmonary blood flow at birth in sheep. *ExpPhysiol* **83**, 833–842.

Iwamoto HS, Teitel D & Rudolph AM (1987). Effects of birth-related events on blood flow distribution. *Pediatr Res* **22**, 634–640.

Kitchen MJ, Habib A, Fouras A, Dubsky S, Lewis RA, Wallace MJ & Hooper SB (2010). A new design for high stability pressure-controlled ventilation for small animal lung imaging. *J Instrum* **5**, T02002.

Kitchen MJ, Paganin D, Lewis RA, Yagi N, Uesugi K & Mudie ST (2004). On the origin of speckle in x-ray phase contrast images of lung tissue. *Phys Med Biol* **49**, 4335–4348.

Lang JA, Pearson JT, te Pas AB, Wallace MJ, Siew ML, Kitchen MJ, Fouras A, Lewis RA, Wheeler K, Polglase GR, Shirai M, Sonobe T & Hooper SB (2014). Ventilation/perfusion mismatch during lung aeration at birth. *J Appl Physiol* **117**, 535–543.

Lewis AB, Heymann MA & Rudolph AM (1976). Gestational changes in pulmonary vascular responses in fetal lambs in utero. *Circ Res* **39**, 536–541.

Morin F & Egan E (1992). Pulmonary hemodynamics in fetal lambs during development at normal and increased oxygen tension. *J Appl Physiol* **73**, 213–218.

Paintal A (1969). Mechanism of stimulation of type J pulmonary receptors. *J Physiol* **203**, 511–532.

Polglase GR & Hooper SB (2006). Role of intra-luminal pressure in regulating PBF in the fetus and after birth. *Curr Pediatr Rev* **2**, 287–299.

Rudolph AM (1979). Fetal and neonatal pulmonary circulation. *Annu Rev Physiol* **41**, 383–395.

Shpilfoygel SD, Close RA, Valentino DJ & Duckwiler GR (2000). X-ray videodensitometric methods for blood flow and velocity measurement: a critical review of literature. *Med Phys* **27**, 2008–2023.

Siew ML, Wallace MJ, Kitchen MJ, Lewis RA, Fouras A, te Pas AB, Yagi N, Uesugi K, Siu KKW & Hooper SB (2009). Inspiration regulates the rate and temporal pattern of lung liquid clearance and lung aeration at birth. *J Appl Physiol* **106**, 1888–1895.

Sobotka KS, Hooper SB, Allison BJ, te Pas AB, Davis PG, Morley CJ & Moss TJ (2011). An initial sustained inflation improves the respiratory and cardiovascular transition at birth in preterm lambs. *Pediatr Res* **70**, 56–60.

Sylvester J, Shimoda LA, Aaronson PI & Ward JP (2012). Hypoxic pulmonary vasoconstriction. *Physiol Rev* **92**, 367–520.

Teitel DF, Iwamoto HS & Rudolph AM (1990). Changes in the pulmonary circulation during birth-related events. *Pediatr Res* **27**, 372–378.

Tiktinsky M & Morin F (1993). Increasing oxygen tension dilates fetal pulmonary circulation via endothelium-derived relaxing factor. *Am J Physiol* **265**, H376–H380.

Weissmann N, Sommer N, Schermuly RT, Ghofrani HA, Seeger W & Grimminger F (2006). Oxygen sensors in hypoxic pulmonary vasoconstriction. *Cardiovasc Res* **71**, 620–629.

Additional information

Competing interests

The authors declare that they have no competing interests.

Author contributions

Conception and design of the experiments: J.A.R.L., J.T.P., R.A.L., S.B.H. Collection, assembly, analysis and interpretation of data: J.A.R.L., J.T.P., C.B., M.J.W., M.L.S., M.J.K., A.B.t.P., A.F., R.A.L., G.R.P., M.S., S.B.H. Drafting the article or revising it critically for important intellectual content: J.A.R.L., J.T.P., C.B., M.J.W., M.L.S., M.J.K., A.B.t.P., A.F., R.A.L., G.R.P., M.S., S.B.H. All authors approved the final version of the manuscript.

Funding

This research was supported by the Australian Research Council, the Australian National Health and Medical Research Council and the Victorian Government's Operational Infrastructure Support Program. We acknowledge travel funding provided by the International Synchrotron Access Program (ISAP) managed by the Australian Synchrotron and funded by the Australian Government. C.B.-H. is supported by the Austrian Science Fund (FWF): J 3595-B19. M.J.K. and A.F. are the recipients of ARC Australian Research Fellowship (DP110101941) and NHMRC Career Development Fellowships, respectively. A.B.tP. is recipient of a Veni-grant, The Netherlands Organisation for Health Research and Development (ZonMw), part of the Innovational Research Incentives Scheme Veni-Vidi-Vici.

Acknowledgements

The authors gratefully acknowledge the support provided by the SPring-8 synchrotron facility (Japan), which was granted by the SPring-8 Program Review Committee, for providing access to the X-ray beamline and associated facilities.

Supporting information

The following supporting information is available in the online version of this article.

Video S1. Simultaneous phase contrast X-ray and angiography recordings in a newborn rabbit (30d gestation) imaged with only the right lung ventilated with 100% N_2 (~30 sec post-ventilation) immediately following birth while the left lung was non-aerated and liquid-filled. Blood vessels are visualized via infusion of iodinated contrast agent; non-aerated regions of the lung are clearly evident by the absence of speckle pattern. The data was acquired at 10 frames per second with a pixel size of 15.3 μm.

Video S2. Simultaneous phase contrast X-ray and angiography recordings in a newborn rabbit (30d gestation) imaged with only the right lung ventilated with 100% O_2 (~30 sec post-ventilation) immediately following birth while the left lung was non-aerated and liquid-filled. Blood vessels are visualized via infusion of iodinated contrast agent; non-aerated regions of the lung are clearly evident by the absence of speckle pattern. The data was acquired at 10 frames per second with a pixel size of 15.3 μm.